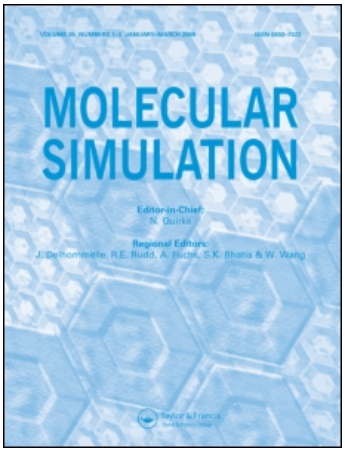

Molecular Simulation
Publication details, including instructions for authors and subscription information:
http://www.informaworld.com/smpp/title~content=t713644482

Molecular Dynamics Simulation of a Langmuir-Blodgett Patch

M. J. Callaway[a]; D. J. Tildesley[a]; N. Quirke[b]
[a] Department of Chemistry, Imperial College of Science, London, U.K. [b] Centre for Computational Chemistry, Department of Chemistry, University of Wales, Bangor Gwynedd, U.K.

To cite this Article Callaway, M. J. , Tildesley, D. J. and Quirke, N.(1996) 'Molecular Dynamics Simulation of a Langmuir-Blodgett Patch', Molecular Simulation, 18: 5, 277 — 301
To link to this Article: DOI: 10.1080/08927029608024125
URL: http://dx.doi.org/10.1080/08927029608024125

Molecular Simulation, 1996, Vol. 18, pp. 277–301
Reprints available directly from the publisher
Photocopying permitted by license only

MOLECULAR DYNAMICS SIMULATION OF A LANGMUIR-BLODGETT PATCH

M. J. CALLAWAY[1], D. J. TILDESLEY[1] and N. QUIRKE[2]

[1]*Department of Chemistry, Imperial College of Science, Technology and Medicine, South Kensington, London SW7 2AY U. K.*
[2]*Centre for Computational Chemistry, Department of Chemistry, University of Wales, Bangor Gwynedd, LL57 2DG, U.K.*

(Received February 1996; accepted August 1996)

The molecular dynamics technique has been used to investigate the structure and stability of an isolated Langmuir-Blodgett patch. The patch consists of 144 stearic acid molecules, modelled using methylene groups with explicit hydrogen atoms and an all-atom representation of the carboxylic acid head group. The molecules are physically adsorbed on a smooth Lennard-Jones substrate with the head groups down. Our results show that the stearic acid patch remains stable when the molecular dynamics simulation at 298 K starts from an energy-minimised structure at a head group area of $A_m = 20.6\,\text{Å}^2\ \text{molec}^{-1}$.

Under these conditions the patch contracts and the stearic acid molecules in the centre of the system form a translational ordered structure at head group area of $A_m = 19.9\ \text{Å}^2\ \text{molec}^{-1}$. At this system size the head-group area of the molecule is 4% lower than that observed experimentally for much larger films. The long axes of the molecules are aligned perpendicular to the surface: on average 97% of molecules have tilt angles of less than 5°. As the patch contracts from its starting configuration there is a slight change in the unit cell. The initial hexagonal structure distorts slightly to form an oblique unit cell with two cell sides differing by 0.35 Å. The vertical orientation of molecules within the patch centre contrasts with significant tilt angles measured by X-ray diffraction for the bulk stearic acid crystals but is supported by recent experimental FTIR observations of the tilt of stearic acid molecules close to a germanium surface.

Keywords: Langmuir-Blodgett patch; stearic acid; physical adsorption

1. INTRODUCTION

When simulating adsorbates on surfaces it is common practice to replicate the system in two dimensions using periodic boundary conditions [1]. This approach removes the effects of patch edges and allows a simulation of a relatively small number of molecules to model a macroscopic adsorbate.

A number of simulations studies of LB monolayers and bilayers have been reported [2, 3, 4, 5, 6, 7]. These simulations have used a variety of potential models to describe the adsorbate-adsorbate and adsorbent-adsorbent interactions but they have all used system with approximately 100 amphiphiles extended in the surface plane using periodic boundary conditions.

This use of the periodic boundary conditions for simulating solid adsorbates can be problematic. In particular, the technique has a tendency to artificially stabilise ordered structures and inhibit large scale molecular rearrangements [8]. This is particularly important when simulating systems with long range translational and orientational ordering since the initial configuration can persist as a metastable state [9] [10].

One can avoid the use of periodic boundary conditions by simulating an isolated patch and then the question of the system size becomes important. Molecules near the edge of a patch experience different forces to those in the centre and a small system may well be unstable. During our previous studies of LB-films we were able to simulate periodic systems of 64 amphiphiles without difficulty [6, 7]. In contrast, when the same model was used to construct an isolated patch of 64 stearic acid molecules in the centre of a much larger simulation cell this system was unstable. The adsorbate patch broke up slowly with molecules falling onto the surface and diffusing in the surface plane with their long-axis parallel to the surface [11]. It was unclear if the instability of the patch was a function of the system size or of the model used to describe the amphiphiles.

The simulation of molecules in an isolated patch offers advantages in the calculation of the long-range forces between the head-groups. For three dimensionally periodic systems containing charges or dipoles, the long-range interactions (i.e. those that fall off more slowly than r^{-D} where D is the dimensionality) are often handled using an Ewald summation. The method includes forces from all of the periodic images of the system in the thermodynamic limit and splits the summation into a real space and reciprocal space interactions.

For adsorbate simulations, with two-dimensional periodicity and a finite extent in the direction perpendicular to the surface, the modifications to the Ewald sum are difficult to implement and the resulting algorithms require a significant amount of computing resource [12]. One advantage of simulating a moderately sized isolated patch is that all the electrostatic interactions can be included by direct summation without the need for an artificial cut-off in the potential or an Ewald sum.

We have simulated an isolated Langmuir-Blodgett patch containing 144 stearic acid molecules. Individual molecules are able to leave the patch, and the patch is able to adopt its most favourable conformation free from any artificial constraints induced by periodic boundary conditions. All of the electrostatic interactions have been included explicitly. In this case the simulation time scales with the square of the number of force sites. In the explicit hydrogen model that we have used to represent the methylene groups of the hydrocarbon chain, there are 53 force sites per amphiphile. The simulation cell contains over 7000 atoms interacting with a static external field. Because of the size of system we have only performed one calculation that took more than 4 months to perform using all of the eight processors of an Alliant FX-80.

This study will help to answer the following questions:

(a) are small patches of amphiphiles adsorbed on surfaces stable?
(b) how does the equilibrium density and translational ordering compare with those of the "infinite" monolayer simulated using periodic boundary conditions?
(c) what is the orientational and conformational ordering of the amphiphiles in the small patch?

Sections 2 and 3 contain a description of the model and the simulation method. Section 4 contains the simulation results and we present our conclusions in section 5.

2. MODEL

The potential model adopted for this simulation has been used successfully in simulation studies of Langmuir-Blodgett monolayers and bilayers [6] [7]. The stearic acid molecule is composed of a methyl tail-group, 16 methylene groups, and a carboxylic acid head-group. All the atoms in the molecule are represented as explicit force sites except the methyl tail-group which is modelled as a single united atom of diameter $\sigma = 3.74$ Å. The bond lengths are constrained to their equilibrium values using the SHAKE algorithm [13], while bond angles are controlled by harmonic potentials of the form

$$V(\theta) = \frac{k_b}{2}(\theta - \theta_0)^2, \tag{1}$$

which are approximated by

$$V(\theta) = k_\theta [1 - \cos(\theta - \theta_0)]. \tag{2}$$

Bond lengths and valence angle potential parameters are given in Table I. The conformation of the hydrocarbon chain is controlled by dihedral potentials of the form proposed by Ryckaert and Bellemans [14]

$$V(\phi) = \sum_{i=0}^{5} c_i (\cos\phi)^i. \tag{3}$$

Four dihedral potentials are used to describe the orientation of the atoms in the head-group with respect to the chain. The dihedral potential parameters are given in Table II. The dispersion interaction between atoms on different molecules, and between atoms separated by three or more backbone sites within a molecule, are modelled through a Lennard-Jones (12–6) potential

$$V(r) = 4\,\varepsilon \left[\left(\frac{\sigma}{r}\right)^{12} - \left(\frac{\sigma}{r}\right)^{6} \right]. \tag{4}$$

The atomic potential parameters are given in Table III. The dipole moment of the carboxylic acid group is represented by four partial charges placed on the head-group atoms. These partial charges produce a molecular dipole moment of 1.79 D in the energy minimised structure. The partial charges in a head-group interact with the partial charges in all other head-groups through a standard coulombic potential.

$$V(r) = \frac{qq'}{4\pi\,\varepsilon_0\, r}. \tag{5}$$

TABLE I Bond-length and bond-angle parameters used to define the geometry of the stearic acid molecule

Bond-length		*Bond-angle*	θ_0	$k_\theta/k\ J\ mol^{-1}$
r_{C-C}/Å	1.53	$<$C—C—C/°	109.5	520
r_{C-H}/Å	1.04	$<$H—C—H/°	1	rigid
r_{C1-O1}/Å	1.364	$<O_1—C_1—$C/°	109	335
r_{C1-O2}/Å	1.25	$<O_2—C_1—$C/°	125	335
r_{O1-H}/Å	0.96	$<O_1—C_1—O_2$/°	124	335
		$<$HD—$O_1—C_1$°	113	146

TABLE II Torsional potential parameters

Torsional	*Potential parameters/kJmol*$^{-1}$
$C_1—C_2—C_3—C_4$	$C_0 = 9.279$
	$C_1 = 12.156$
	$C_2 = -13.120$
	$C_3 = -3.058$
	$C_4 = 26.240$
	$C_5 = -31.495$
$O_1—C_1—C_2—C_3$	$C_0 = -0.151$
	$C_1 = -0.353$
	$C_2 = -0.300$
	$C_3 = -0.204$
$O_2—C_1—C_2—C_3$	$C_0 = 0.597$
	$C_1 = -0.2435$
	$C_2 = -0.904$
	$C_3 = -0.300$
$HD—O_1—C_1—C_2$	$C_0 = 0.500$
	$C_1 = 0.000$
	$C_2 = -0.500$
	$C_3 = 0.000$
$HD-O_1-C_1-O_2$	$C_0 = 3.958$
	$C_1 = 1.643$
	$C_2 = -5.600$
	$C_3 = 0.000$

TABLE III Potential parameters for atoms in the stearic acid molecule

Site	$\varepsilon/kJ\ mol^{-1}$	$\sigma/\AA$	*mass/amu*	$q_\alpha/\lvert e\rvert$
CH_3	0.64230	3.740	15.035	–
C	0.405610	2.908	12.011	–
H	0.05683	2.908	1.008	–
C_1	0.50209	3.296	15.035	0.575
O_1	0.62760	2.940	15.995	−0.350
O_2	0.83683	2.850	15.995	−0.450
H(D)	0.08368	1.782	2.016	0.225

All atoms in the patch interact with a structureless supporting surface through an integrated Lennard-Jones (9–3) potential

$$V(z) = \frac{2\pi\rho\varepsilon\sigma^3}{3}\left[\frac{2}{15}\left(\frac{\sigma}{z}\right)^9 - \left(\frac{\sigma}{z}\right)^3\right], \tag{6}$$

where ρ the number density of the substrate is set to 0.114 $\AA^{-3}$, appropriate for graphite. The surface potential parameters are set to $\varepsilon/k_B = 28$ K and $\sigma = 3.4$ Å in the simulation.

The head-group charges, q_c, induce a corresponding set of image-charges, q_i, in the supporting substrate. Each charge interacts with all the induced image-charges through a potential of the form

$$V_{ic} = \frac{1}{2} \frac{q_c q_i}{(4\pi \varepsilon_0) 2(z_i - z_p)}, \tag{7}$$

where z_i is the height of the charge and z_p is the height of the image-plane above the surface, set to a value of $\sigma_{ss}/2$ or 1.7 Å for this study. The size of the image charge is

$$q_i = \left[\frac{\varepsilon - \varepsilon'}{\varepsilon + \varepsilon'}\right] q_c, \tag{8}$$

where ε is the dielectric constant of the vacuum and ε' the dielectric constant of the surface is set to 4.

3. THE SIMULATION

The Langmuir-Blodgett patch is constructed from a hexagonally close packed array of 12×12 stearic acid molecules oriented so that the carboxylic acid head-groups are close to the surface. No force cut-off was applied for the calculation of the non-bonded and charge-charge intermolecular interactions. The simulation was started from an energy minimised structure with an initial head-group area of $A_m = 20.6\,\text{Å}^2$ molec^{-1} and the system thermalised by randomly assigning velocities to particles from a Maxwell-Boltzmann distribution at room temperature. The net linear and angular momentum of the patch were calculated at the start of the simulation and set to zero. It is essential to remove the angular momentum for a patch to avoid the rotation of the entire structure on the surface. This motion which is inhibited in periodic boundary conditions occurs readily for an isolated patch. The method of removing the net angular momentum is described in the appendix. The system was equilibrated at a temperature of 298 K for 5×10^4 timesteps, or 100 ps. Following the equilibration cycle, a production cycle of 2×10^4 timesteps, 40 ps, was performed. 1×10^3 timesteps takes approximately 28 hrs running in parallel on an 8 processor cluster of an Alliant FX-80.

4. RESULTS

The patch remained stable over the duration of the simulation, 140 ps. In Figure 1 we present a side view of the final configuration using a space-filling representation of the molecules. On the left hand-side of the picture one molecule has partially slipped down the side of the patch. This occurred at several points in the simulation. The molecules appeared stable in this configuration, at no point in the simulation did these molecules completely leave the edge of the patch.

Figures 2, 3 and 4 show projections of the positions of head-groups, molecular centres of masses, and tail-groups on to the plane of the surface during the last 10 ps of the simulation. Each point represents the instantaneous position of the centres, tails and head taken at equal time intervals during the end of the production phase. The centres of mass are more highly ordered than the heads or the tails of the amphiphiles. While the head-groups of some molecules on the edge of the patch can be seen to be wandering on the supporting surface the corresponding tail-groups are more rigidly bound to the patch. The analysis of the next section shows that in the centre of the patch the head groups are slightly more ordered than the tails. From the positions of the centre of masses, Figure 3, it can be seen that the patch has rearranged into two separate domains with a slightly

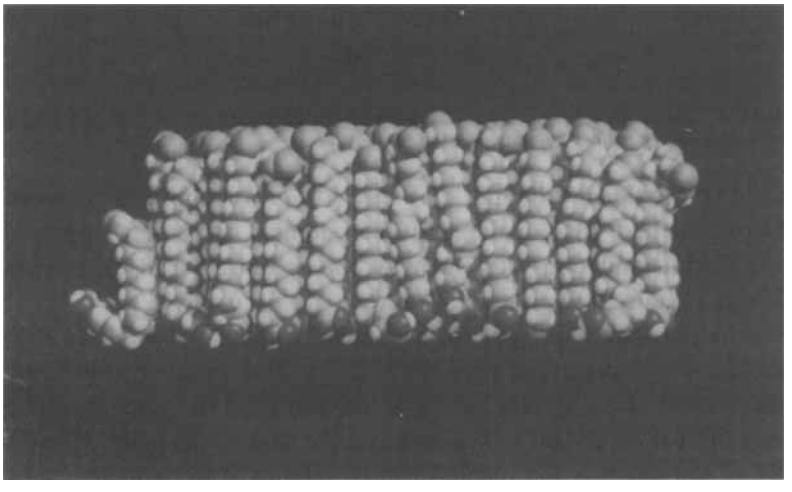

FIGURE 1 A side view of the final configuration of the Langmuir-Blodgett patch using a space filling representation of the molecules. The oxygens of the head group are red and the hydrogen atoms white. See COLOR PLATE I.

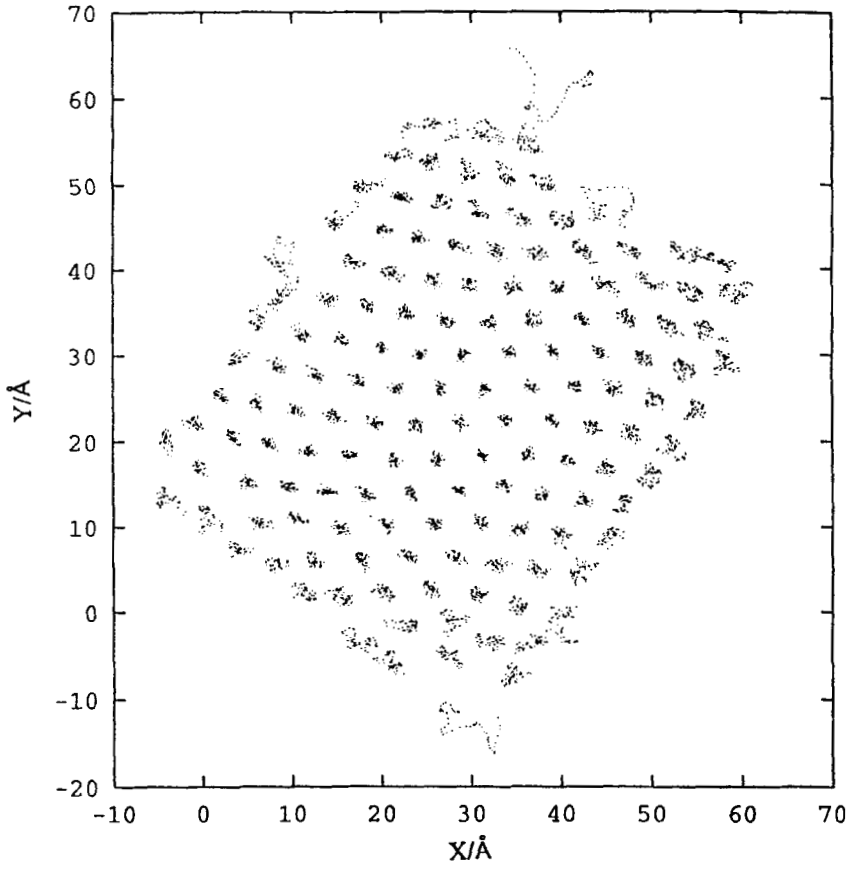

FIGURE 2 The projected positions of the molecular head-groups on the surface plane during the final 10 ps of the production phase of the simulation.

different translational ordering. This observation corroborates observations of Siepmann and McDonald [15] that domain structures appeared in Monte Carlo simulations of systems of 100 or more hexadecyl mercaptan molecules chemisorbed on a gold surface.

For the purpose of analysis we have divided the patch into two regions. Molecules whose centres of mass lie within a 20 Å radius cut-off from the centre of mass of the system belong to the centre of the patch, while those outside this cut-off are treated as being on the edge of the patch. Clearly the centre of the patch is the region of most interest if we wish to relate the structure of the patch to that of the periodic film. A 20 Å cut-off maximises the number of molecules within this region for statistical sampling while excluding the most highly disordered molecules on the edge of the patch.

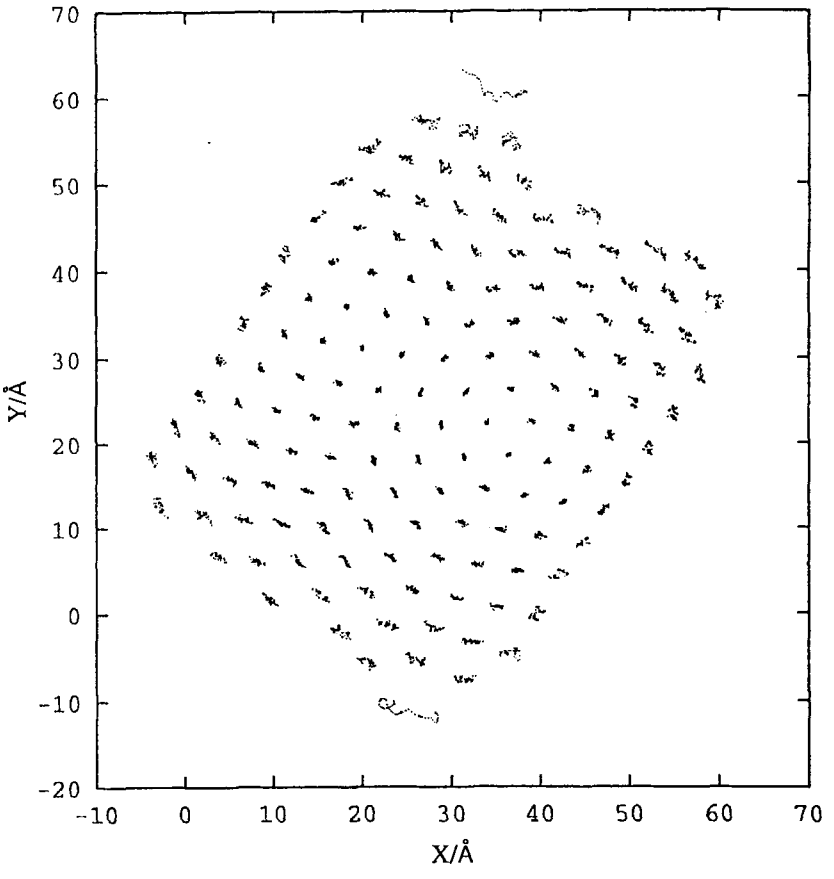

FIGURE 3 The projected positions of the molecular centres of masses on the surface plane during the final 10 ps of the production phase of the simulation.

Figure 5 shows the head-group area per molecule, $A_m(r)$, of the patch as a function of cut-off distance, r, from the centre of mass of the patch. The limiting behaviour as r approaches 20 Å should provide an estimate of the head-group area per molecule in the patch. The head group area per molecule is the inverse of the two dimensional number density. The extrapolated value of $A_m = 19.9$ Å^2 molec^{-1} lies just inside the steeply rising portion of the Π-A_m adsorption isotherm for a Langmuir film of stearic acid on water [16]. This corresponds to a significant positive spreading pressure on water for an effectively infinite film of amphiphiles. For this model of stearic acid the small patch adsorbed on a solid is at zero spreading pressure. This small decrease in the equilibrium head group area from 20.6 (the value predicted by

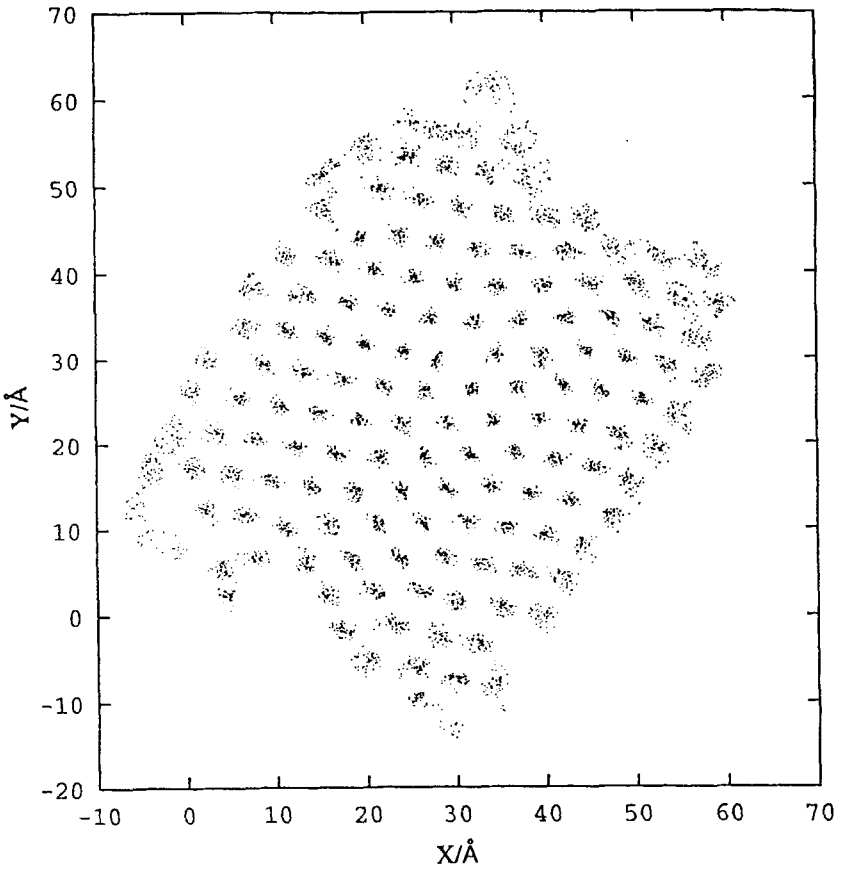

FIGURE 4 The projected positions of the molecular tail-groups on the surface plane during the final 10 ps of the production phase of the simulation.

energy minimisation studies of model periodic films) to 19.9 Å^2 molec^{-1} must be related to the small size of the patch.

It is instructive to compare this calculated packing density with experimentally measured values. X-ray diffraction measurements on single crystals of stearic acid, have revealed two-dimensional densities within the crystals layers. These are $A_m = 20.6$ Å^2 molec^{-1} for the E form [17], $A_m = 20.7$ Å^2 molec^{-1} for the B form [18] and $A_m = 23.2$ Å^2 molec^{-1} for the C form [19]. Electron diffraction measurements of cadmium stearate Langmuir-Blodgett films on a silica substrate gave a coverage (the inverse of the two dimensional number density) of $A_m = 20.7$ Å^2 molec^{-1} [20]. The head group area of the simulated patch is approximately 4% lower than the experimental head-group area for much larger systems. While this agreement is gratifying, it is

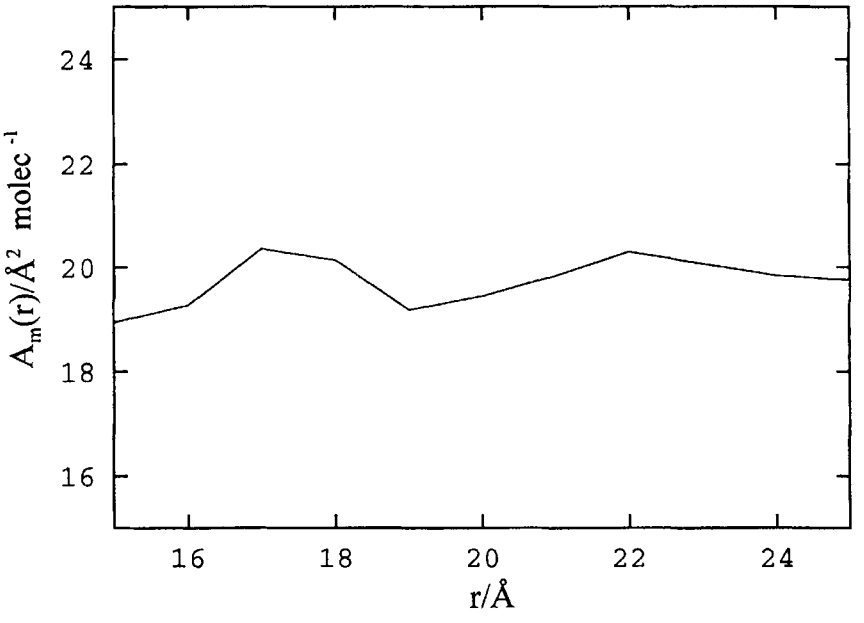

FIGURE 5 The time-averaged molecular density as a function of the cut-off radius measured from the centre of mass of the patch.

difficult to be certain whether the remaining discrepancy is caused by inaccuracies in the model or by the size of the patch. It would be interesting but expensive to monitor patch density using different sizes of patch. On the other hand it might be possible to evaluate the spreading pressure for a monolayer at a fixed density using a periodic simulation. This would require an accurate estimate of the normal and tangential components of the pressure in the layer which is an expensive additional calculation.

Translational Order

We have monitored the degree of translational ordering by calculating the hexatic order parameter

$$O_6 = \frac{1}{6N} \left\langle \sum_{i=1}^{N} \sum_{i=1}^{6} \exp(6i\phi_j) \right\rangle \tag{9}$$

where there are N molecules in the centre of the patch and ϕ_j is the angle between the vectors from a molecule i to two of its nearest neighbours j. There are six angles associated with a molecule i and the value of ϕ_j in the

perfect triangular lattice is $\pi/6$ giving $O_6 = 1.0$. The averaged hexatic order parameters O_6 in the centre of the patch is 0.71 for head-groups, 0.84 for centre of masses, and 0.65 for tail-groups, confirming the high degree of translational ordering. A periodic film of density $A_m = 20.6$ Å^2 molec^{-1} at the same temperature had an order parameter O_6 of 0.81 for centre of masses and 0.56 for tail-groups. The value of O_6 varied little during the production phase of the simulation, Figures 6(a–c), demonstrating the stability of the lattice structure.

This analysis assumes that the translational structure retains its original hexagonal structure and that O_6 is the appropriate order parameter. We have checked this by calculating the two dimensional radial distribution function $g(r)$ of corresponding to different parts of the amphiphile. In this calculation the relevant atoms are projected on to a surface plane and the distance r is measured in the plane. The radial distribution of head-groups and methyl tail-groups are characteristic of a solid hexagonal structure and we have not reproduced them in the paper. The height of the nearest neighbour peak is 3.5 in the case of the tail-groups. This greater than the primary peak in an equivalent periodic system at a head-group area of $A_m = 20.6$ Å^2 molec^{-1}, which is 3 for the tail-groups.

In the radial distribution function of the centres of mass, Figure 7(a), the first maximum is split into two and the second maximum into four subpeaks. The additional structure within the radial distribution function can be explained if the translational structure of the patch changes to produce an oblique unit cell with ($|\mathbf{a}| = 4.45$ Å, $|\mathbf{b}| = 4.8$ Å and $\phi = 68.7°$. (The unit cell parameters are estimated by fitting to the radial distribution function). This reordering is illustrated in Figure 7(b) where we show the centre of mass positions in the final configurations. Nearest neighbour separations less than 4.6 Å are shown as solid lines and the new unit cell structure can be inferred from the figure.

Calculation of the structure factor, $S(\mathbf{k})$ for a system provides an alternative method of looking at underlying symmetry of the patch.

$$S(\mathbf{k}) = \frac{1}{N}\langle \rho_k \cdot \rho_{-k} \rangle \tag{10}$$

where for N amphiphiles containing m scattering centres

$$\rho_{\mathbf{k}} = \sum_{i=1}^{N} \sum_{\alpha=1}^{m} b_\alpha(|\mathbf{k}|) \exp(i\mathbf{k} \cdot \mathbf{r}_{i\alpha}) \tag{11}$$

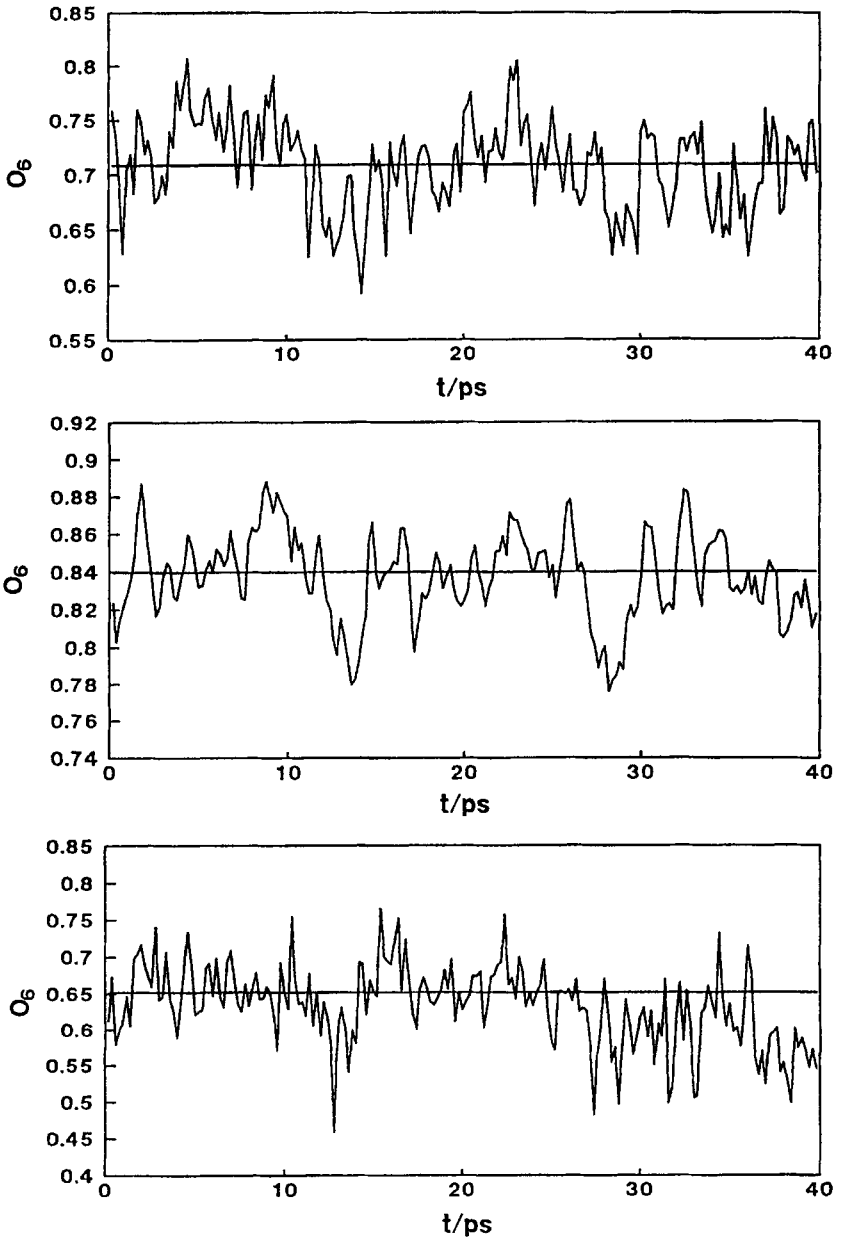

FIGURE 6 The variation in the hexatic order parameter over the production phase of the simulation: (a) head-groups; (b) molecular centres of masses; (c) tail-groups.

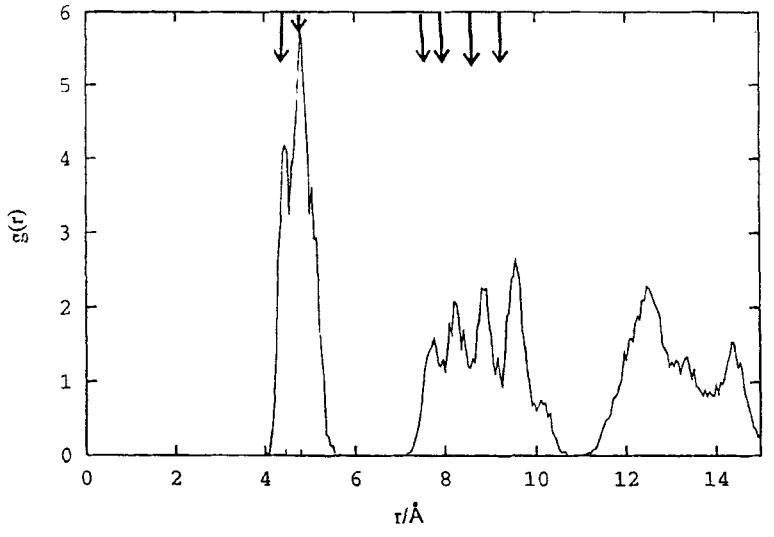

(a)

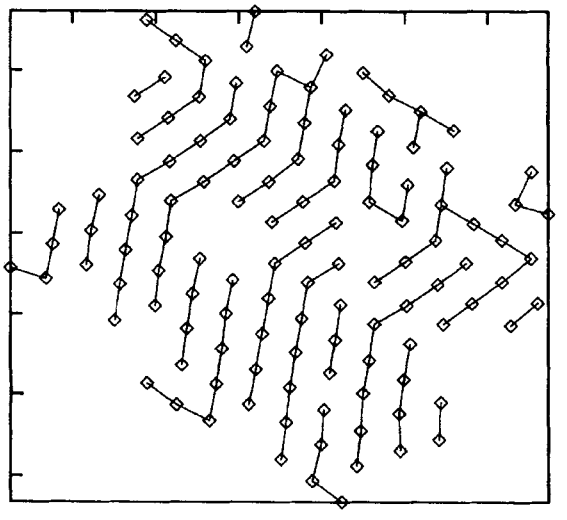

(b)

FIGURE 7 (a) The two-dimensional radial distribution function of the molecular centres of mass, $g(r)$, averaged over the production cycle. The splittings in the first two peaks are marked with vertical arrows. (b) An instantaneous snap-shot of the molecular centres of mass for the 118 amphiphiles in the centre of the patch. Nearest neighbour separations of less than 4.6 Å are shown as solid lines.

and $b_\alpha(|\mathbf{k}|)$ is the X-ray scattering length of the scattering atom. Figure 8(a) shows the structure factor from the film at room temperature compared with the structure factor of the starting configuration, Figure 8(b), in which

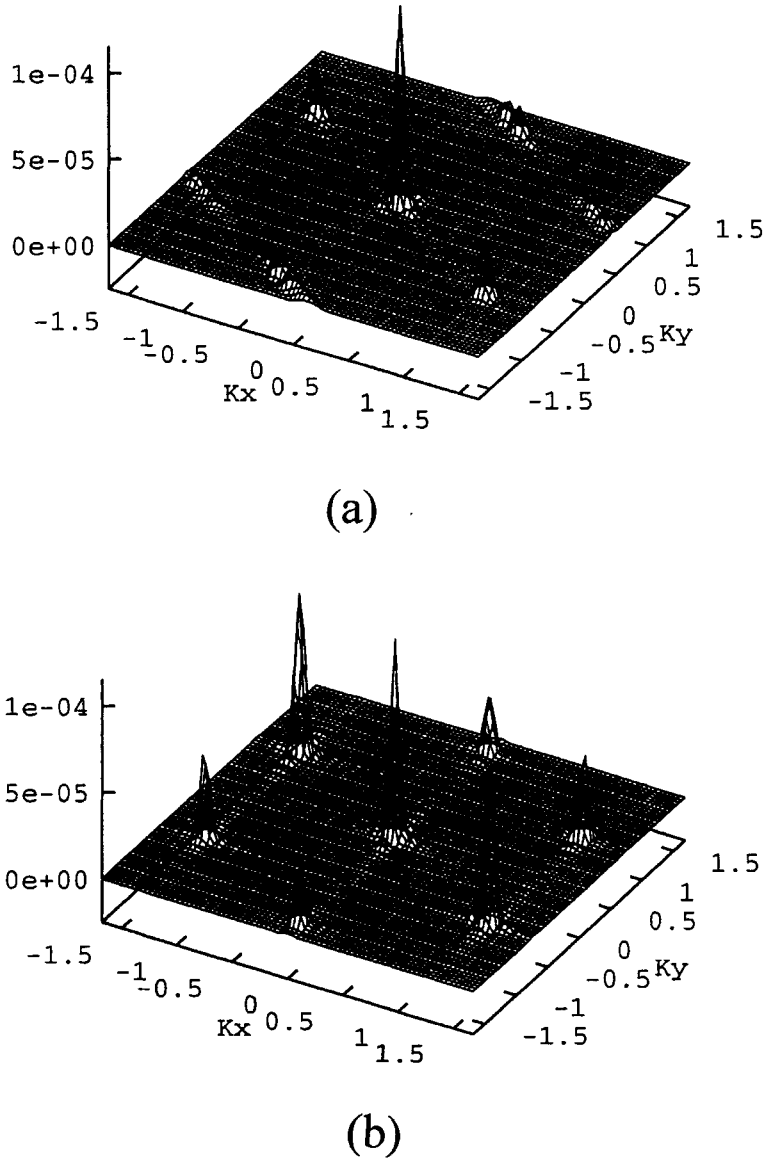

FIGURE 8 The structure factor S(k): (a) the thermalized Langmuir-Blodgett patch; (b) the ideal hexagonal lattice starting configuration.

molecules are arranged in an hexagonal lattice and orientated along the surface normal. The relative sizes and positions of the peaks, two strong and four slightly weaker, are similar in each case. The broadening of the peaks in Figure 8(a) is associated with the thermal motion of the lattice and the slight distortion in the lattice structure. Interestingly, the ideal structure has the 2 strong peaks and four weak peaks. This variation is normally ascribed to some tilting of the amphiphiles with respect to the surface normal but in this system the molecules are perfectly normal to the surface and the variation must be the effect of the alignment of the molecular backbones (the short axis of the molecule) in the starting configuration and the thermalized configuration.

Orientational Order

Figure 9(a) shows the time averaged mean tilt angle, $n(\cos(\theta))$, and Figure 9(b) shows the azimuthal angle distribution, $n(\phi)$ for molecules in the centre of the patch. The tilt angle θ is measured relative to the surface normal. During the production phase 97% of molecules are oriented within 5° of the vertical. In orientations close to the vertical small changes to the in-plane components of the ordering vector can make large changes to the azimuthal angle. As one would expect molecules within the patch show little preference for any a particular azimuthal orientation, and $n(\phi)$ is almost evenly distributed across 2π radians.

Within the centre of the patch any conformational disorder is mainly restricted to the region of the head-groups and tail-groups. If we define gauche plus and gauche minus defects as dihedral angles in the ranges 0° to 120° and 240° to 360° respectively, then the number of all-trans molecules within the centre of the patch is 96.3%. In an equivalent periodic film, at a density of $A_m = 20.6$ Å^2 molec^{-1}, 97.7% of molecules are in an all-trans configuration [21].

Dipolar Orientation

Charges in the stearic acid molecule are concentrated on the atoms of the carboxylic acid head-group. The close packing of these head-groups within Langmuir-Blodgett films leads to significant charge interactions both between molecules, and with the image-charges induced in the polarisable substrate. Inclusion of these electrostatic interactions, which contribute more than 25% of the energy of the total energy of the patch.

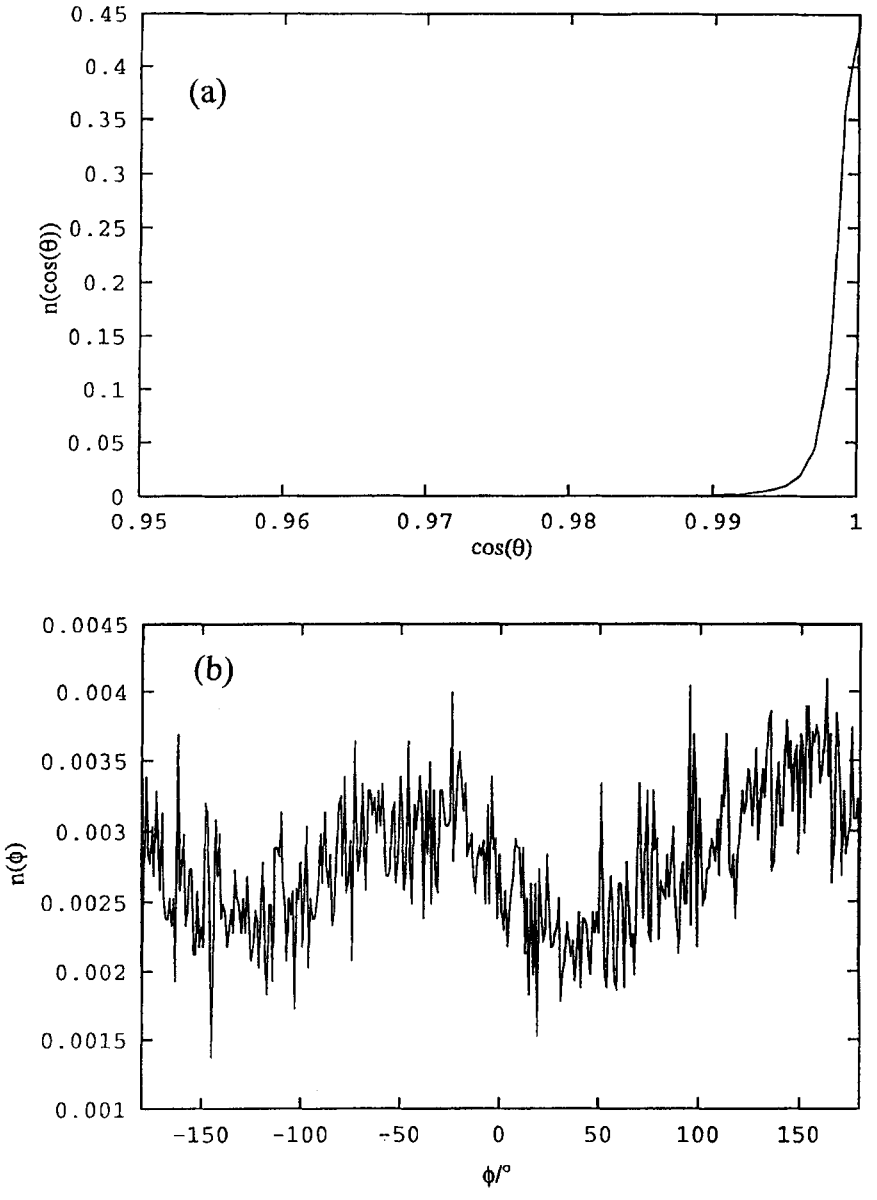

FIGURE 9 (a) The normalised distribution of molecular tilt angles, $n(\cos(\theta))$. (b) Normalised distribution of molecular azimuthal angles, $n(\phi)$.

The four point charges within each carboxylic acid head-group may be represented as single dipole. The dipole vector, $\boldsymbol{\mu}$, is defined as

$$\boldsymbol{\mu} = \sum_{i=1}^{4} q_i \mathbf{r}_i, \tag{12}$$

and acts approximately parallel to the C=O bond, directed from the oxygen atom to the carbon, with a mean magnitude of 1.66 D. Figures 10(a–b) shows the time averaged distribution of the dipolar tilt angle, cos (θ_μ), and azimuthal angle, ϕ_μ. Dipoles within the patch are orientated principally parallel to the surface, 46% are within 10°, this in-plane orientation is driven by strong charge image-charge, interactions with the surface. The second smaller peak on the right hand side of the plot corresponds to dipoles tilted down towards the surface. This second peak is also seen the equivalent periodic system, although it is less pronounced. It may in part be due to the repulsive effects of dipoles aligned in anti-parallel orientations, head-to-head and tail-to-tail.

The dipolar azimuthal angle is less sharply defined than the tilt angle, forming a single broad maxima approximately 100° wide. This broad peak is observed in an equivalent periodic system, $A_m = 20.6$ Å^2 molec^{-1}, and arises from competition between the aligning forces of the dipoles and rotation about the long axis of the stearic acid molecules. The patch has an average dipole, M of 0.699 D per molecule, which varied little during the production phase of the simulation. The time dependence of the total dipole moment of the patch is shown in Figure 11. The starting configuration in which molecular dipoles are aligned along common axis has a dipole moment M of magnitude 1.69 D per molecule.

Figure 12 shows dipole vectors at the final simulation step projected on to the plane of the surface, dipole vectors are displayed centred on the carbon atom in the carboxylic acid head-group. The figure shows that the majority of dipoles are aligned head-to-tail.

5. DISCUSSION

Energy minimisation studies of stearic acid monolayers have already shown that important structural properties such as the molecular tilt angle and the lattice structure are highly dependent on packing density [6]. Simulating an isolated patch of molecules allows us to investigate the natural state of a small Langmuir-Blodgett patch without the influence of periodic boundary conditions. We have simulated a monolayer of 144 stearic acid molecules on a graphite surface without periodic boundary conditions. On the simulation timescale, 140 ps, the system was stable, no molecules left the edge of the

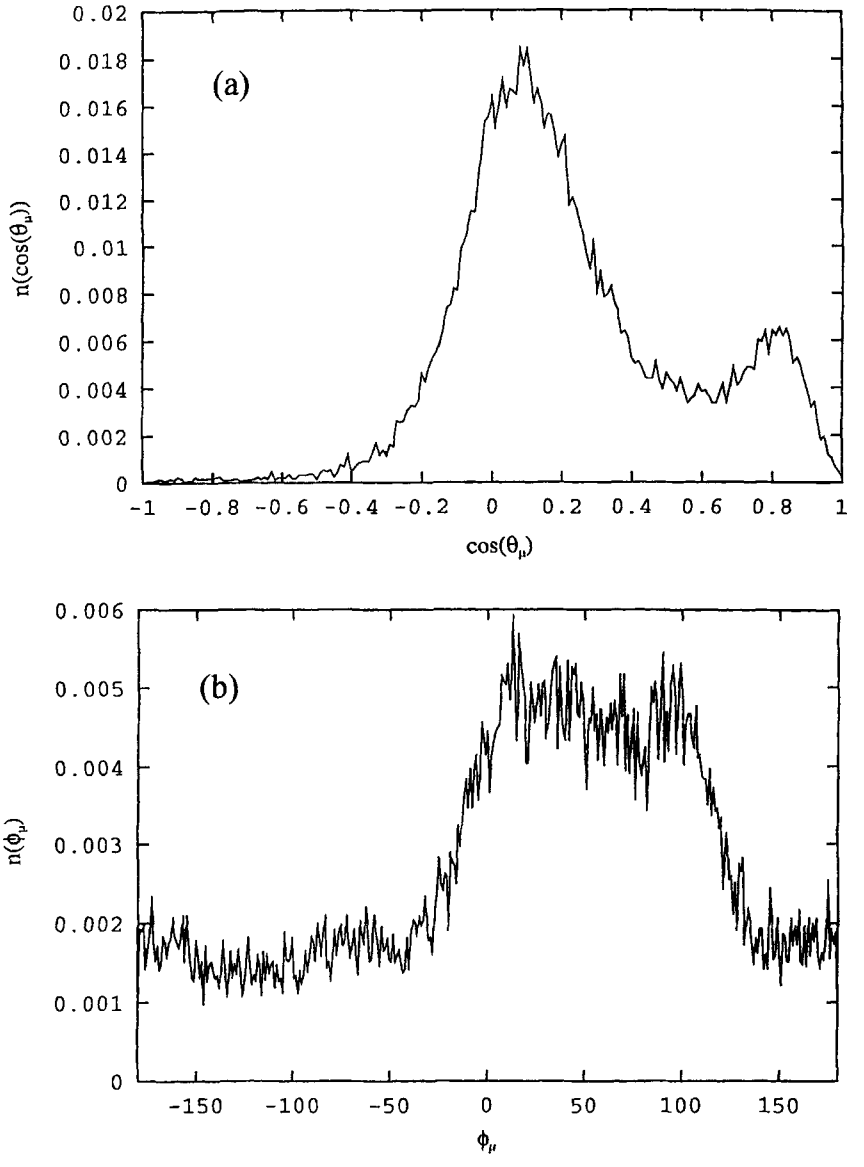

FIGURE 10 (a) The normalised distributions of the dipole orientation, $n(\cos(\theta_\mu))$. (b) Normalised distribution of dipolar azimuthal angles, $n(\phi_\mu)$.

patch and the molecules remained essentially perpendicular to the surface. The patch underwent a small contraction. A patches containing 144 amphiphiles appears to be stable, while our previous study suggests that a smaller systems containing 64 molecules were unstable, collapsing on to the surface.

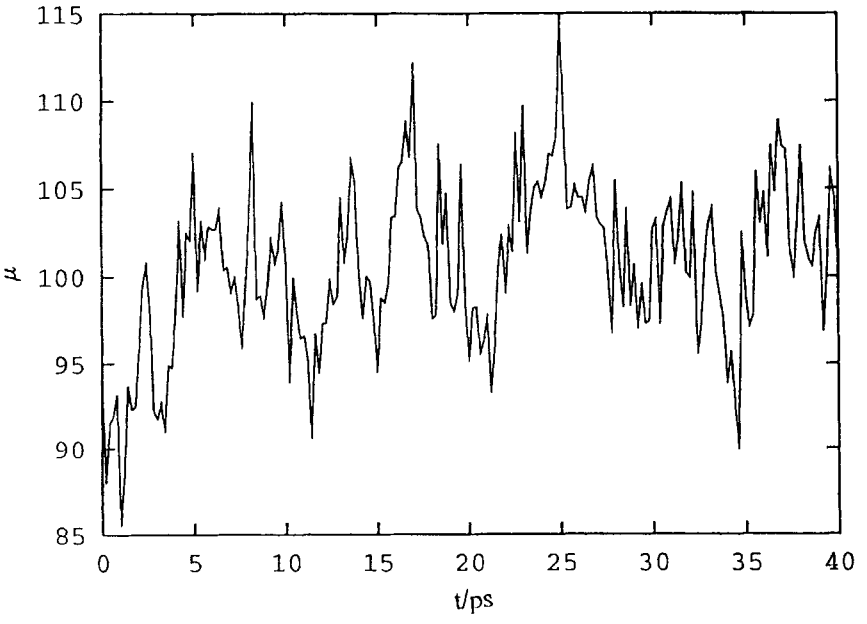

FIGURE 11 The variation in the total dipole moment of the Langmuir-Blodgett patch in the production phase of the simulation.

There is a clear distinction between molecules in the centre of the patch which remain highly ordered, and the more conformationally disordered molecules on the outer edge. Stearic acid molecules outside a 20 Å spherical cut-off from the patch centre contained over twice the total number of gauche defects of those inside the cut-off, and over thirteen times the number of gauche defects in the alkyl chain, i.e. excluding the head-group and tail-groups torsions where most defects occur.

The stearic acid molecules in the centre of the system form a high density, ordered structure, $A_m = 19.9$ Å^2 molec^{-1}. At this system size the head-group area molecule is 4% lower than that observed experimentally for much larger films. The long axes of the molecules are aligned perpendicular to the surface: on average 97% of molecules have tilt angles of less than 5°. As the patch contracts from its starting configuration there is a slight change in the unit cell. The initial hexagonal structure distorts slightly to form an oblique unit cell with two cell sides differing by approximately 0.35 Å. This behaviour is not observed in the simulations of the films with periodic boundary conditions. In reference [7] there is no observable splitting in the centre of mass radial distribution function. This may well be a problem associated with the fixed periodic boundary conditions where any translational structural changes

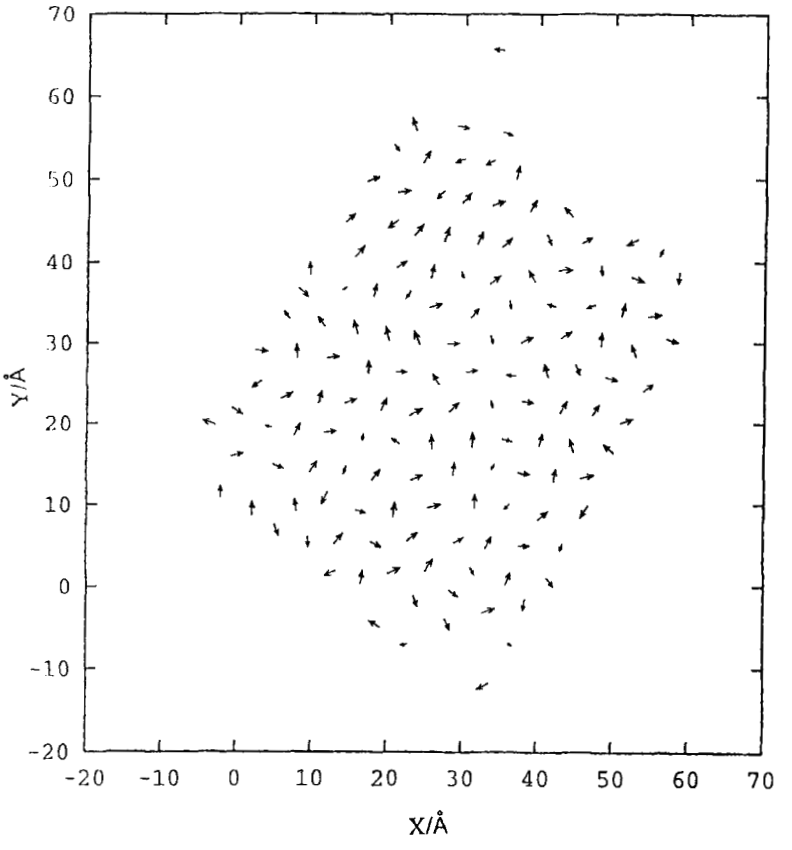

FIGURE 12 The projection of the molecular dipole vectors on the surface plane. Dipole vectors are displayed centred on the carbon atom of the carboxylic acid head-group. The longer vectors correspond to dipoles pointing along the plane of the surface. The shorter vectors correspond to dipoles aligned out of the plane of the surface.

must be artificially commensurate with the simulation box. A rectangular distortion of 0.35 Å in a lattice spacing of 4.8 Å is difficult to accommodate in an 8×8 lattice. The use of the patch geometry is the obvious way to simulate these changes but we have to be aware that an increase in density may also be caused by the small size of the patch.

The high degree of orientational ordering in the central region of the simulated Langmuir-Blodgett patch must be strongly coupled to the increase in the density over the periodic film. It is interesting that similar orientational distributions are obtained both for the patch and the periodic film. It appears that the periodic boundary conditions do not artificially stabilize the orientational ordering of the amphiphiles in this case.

The vertical orientation of molecules within the patch centre contrasts with significant tilt angles measured by X-ray diffraction of bulk stearic acid crystals. The B and E crystal structures have similar in-plane packing densities, 20.7 $Å^2$ $molec^{-1}$ and 20.6 $Å^2$ $molec^{-1}$, to the monolayer but have molecular tilts of 27° and 26° respectively.

This observation supports the experimental observations of monolayer Langmuir-Blodgett films. It is generally accepted that the structure of thin Langmuir-Blodgett films is affected by the presence of the substrate and that increasing the depth of a film causes a transition towards the bulk crystal structure. Kimura, Umemura and Takenaka have studied stearic acid Langmuir-Blodgett films on a germanium substrate using FTIR-ATR [22]. They observed that the hydrocarbon chains in first monolayer are packed in hexagonal or pseudohexagonal subcells with the chain axis orientated perpendicular to the surface. Increasing the depth of the film caused the system to crystallize into the monoclinic structure, with a tilt angle of about 30° in the case of the C-form [22].

Schwartz *al.* have used atomic force microscopy to study different depth Langmuir-Blodgett films. They report that monolayer films of manganese arachidate and lead stearate have different lattice structures to the equivalent multilayer films. Increasing the depth of the lead stearate film to seven layers causes the lattice dimensions to change to values approaching those of the bulk crystal [23]. This difference in behaviour is almost certainly due to the different requirements for a strong hydrogen bonding interaction between two carboxylic acid groups and between one carboxylic acid group and the surface. In our model the charges of the head-group induce images in the surface that are not connected to a particular hydrocarbon chains and are free to orient in the surface.

Acknowledgements

We wish to thank BP Research, Sunbury-on-Thames, for a CASE award for MJC. DJT acknowledges useful discussions with David Fincham. We wish thank the EPSRC for a grant GR/J/74459 for the purchase of computing equipment.

APPENDIX. REMOVAL OF ANGULAR MOMENTUM

Following a suggestion from David Fincham, Keele University, we remove the angular momentum of the patch in the following way.

The total angular momentum, **L**, of a system of particles, i, of masses m_i and at positions $\mathbf{r}_i$, is defined by the expression,

$$\mathbf{L} = \sum_i \mathbf{r}_i \times \mathbf{p}_i, \tag{13}$$

which may be rewritten as,

$$\mathbf{L} = \sum_i (\mathbf{R} + \mathbf{r}_i^*) \times \mathbf{p}_i, \tag{14}$$

where **R** is the position of the centre of mass of the patch and $\mathbf{r}^*$ is the position of particle i relative to the centre of mass. If the total linear momentum of the system is zero, then the term

$$\mathbf{R} \times \sum_i \mathbf{p}_i = 0, \tag{15}$$

and the total angular momentum acting about the centre of mass is,

$$\begin{aligned} \mathbf{L} &= \sum_i \mathbf{r}_i^* \times \mathbf{p}_i \\ &= \sum_i \mathbf{r}_i^* \times m_i \mathbf{v}_i \\ &= \sum_i \mathbf{r}_i^* \times (m_i \boldsymbol{\omega} \times \mathbf{r}_i^*) \end{aligned} \tag{16}$$

The angular momentum of the patch is

$$\boldsymbol{\omega} = \mathbf{I}^{-1} \cdot \mathbf{L}, \tag{17}$$

where the rotational inertia matrix, **I**, is

$$I_{\alpha\beta} = \sum_i m_i (\delta_{\alpha\beta} \mathbf{r}_i^{*2} - r_{\alpha i}^* r_{\beta i}^*) \tag{18}$$

where α and β are the Cartesian indices and $\delta_{\alpha\beta}$ is the Kronecker delta.

The corrected atomic velocities, $\mathbf{v}_i'$ corresponding to zero angular momentum of the patch are given by

$$\mathbf{v}_i' = \mathbf{v}_i - \boldsymbol{\omega} \times \mathbf{r}_i^*. \tag{19}$$

This easily demonstrated by substituting eqn (19) into eqn (16) to obtain the new angular momentum

$$\begin{aligned} \mathbf{L}' &= \sum_i m_i \mathbf{r}_i^* \times (\mathbf{v}_i - \boldsymbol{\omega} \times \mathbf{r}_i^*) \\ &= 0 \end{aligned} \tag{20}$$

References

[1] Allen, M.P. and Tildesley, D. J. (1987). *Computer Simulation of Liquids* Oxford: Clarendon press.

[2] Cardini, G., Bareman, J. P. and Klein, M. L. (1988). "Characterisation of a Langmuir-Blodgett monolayer using molecular dynamics calculations", *Chem. Phys. Letts.*, **145**, 493.

[3] Hautman, J., Bareman, J. P., Mar, W. and Klein, M. L. (1991). "Molecular-dynamics investigations of self-assembled monolayers," *J. Chem. Soc. Faraday Trans.*, **87**, 2031.

[4] Mar, W. and Klein, M. L. (1994). "Molecular-dynamics study of the self-assembled monolayer composed $CS(CH_2)$ (14) CH_3 molecules using an all-atoms model", *Langmuir*, **10**, 188.

[5] Sprik, M., Delmarche, E., Michel, B., Röthlisberger, U., Klein, M. L., Wolf, H. and Ringsdorf, H. (1994). "Structure of hydrophilic self-assembled monolayers – A combined scanning-tunneling-microscopy and computer-simulation study," *Langmuir*, **10**, 4116.

[6] Kim, K. S., Moller, M. A., Tildesley, D. J. and Quirke, N. (1994). "Molecular-dynamics simulations of Langmuir-Blodgett monolayers with explicit headgroup interactions," *Mol. Sim.*, **13**, 77.

[7] Kim, K. S., Tildesley, D. J. and Quirke, N. (1994). "Molecular-dynamics simulations of Langmuir-Blodgett-Films. 2. Bilayers," *Mol. Sim.*, **13**, 101.

[8] Strandburg, K. J. (1988). "Two dimensional melting," *Reviews of Modern Physics*, **60**, 161.

[9] Pratt, L. R. and Haan, S. W. (1981). "Effects of Periodic Boundary-conditions on equilibrium properties C Computer-simulated Fluids .1. Theory," *J. Chem. Phys.*, **74**, 1864.

[10] Impey, R. W., Madden, P. A. and Tildesley, D. J.(1981). "On the calculation of the orientational correlation parameter G2," *Mol. Phys.*, **44**, 1319.

[11] Bowles, R. T. (1990). Unpublished simulation results.

[12] Tildesley, D. J. (1993). *Computer Simulation in Chemical Physics*, Allen, M. P., Tildesley, D. J. Eds. Kluwer: Boston, MA, Chapter 2.

[13] Ryckaert, J. P., Ciccotti. G. and Berendsen, H. J. C. (1977). "Numerical integration of the cartesian equations of motion of a system with constraints: Molecular dynamics of n-Alkanes" *J. Comput. Phys.*, **23**, 327.

[14] Ryckaert, J. P. and Bellemans, A. (1975). "Molecular dynamics of liquid n-butane near its boiling point" *Chem. Phys. Lett.*, **30**, 123.

[15] Seipmann, J. I., McDonald, I. R. (1993). Domain formation and system-size dependence in simulations of self assembled monolayers, *Langmuir*, **9**, 2351.

[16] Roberts, G. G. (1985). "An applied science perspective of Langmuir-Blodgett films," *Adv. Phys.*, **34**, 475.

[17] Kaneko, F., Kobayashi, S., Kitagawa, Y. and Matsuura, Y. (1990). "Structure of stearic-acid E-form," *Acta Cryst.*, **C46**, 1490.

[18] Goto, M. and Asada, E. (1978). "The crystal structure of the B-form of stearic acid *Bull. Chem. Soc. Jpn.*, **51**, 2456.
[19] Malta, V., Celotti, G., Zannetti, R. and Martella, A. F. (1971). "Crystal structure of the C form of stearic acid *J. Chem. Soc.*, **B3**, 548.
[20] Garoff, S., Deckmann, H. W., Dunsmuir, J. H., Alverez, M. S. and Bloch, J. M. (1986). "Bond-orientational order in Langmuir-Blodgett surfactant monolayer," *J. Phys.*, **47**, 701.
[21] Kim, K. S. (1991). Ph.D. Thesis, University of Southampton, 135.
[22] Kimura, F., Umemura, J. and Takenaka, T. (1986). "FTIR-ATR studies on Langmuir-Blodgett films of Stearic-acid with 1 monolayers," *Langmuir*, **2**, 96.
[23] Schwartz, D. K., Viswanathan, R., Garnaes, J. and Zasadzinski, J. A. N. (1993). "Influence of cations, alkane chain-length, and substrate on molecular order of Langmuir-Blodgett-films," *J. Am. Chem. Soc.*, **115**, 7374.